

## RESEARCH OUTPUTS / RÉSULTATS DE RECHERCHE

### Tuneable Emission of Polyhedral Oligomeric Silsesquioxane Based Nanostructures that Self-Assemble in the Presence of Europium(III) Ions

Cinà, Valerio; Carbonell, Esther; Fusaro, Luca; García, Hermenegildo; Gruttadauria, Michelangelo; Giacalone, Francesco; Aprile, Carmela

*Published in:*  
ChemPlusChem

*DOI:*  
[10.1002/cplu.201900575](https://doi.org/10.1002/cplu.201900575)

*Publication date:*  
2020

*Document Version*  
Peer reviewed version

[Link to publication](#)

*Citation for published version (HARVARD):*

Cinà, V, Carbonell, E, Fusaro, L, García, H, Gruttadauria, M, Giacalone, F & Aprile, C 2020, 'Tuneable Emission of Polyhedral Oligomeric Silsesquioxane Based Nanostructures that Self-Assemble in the Presence of Europium(III) Ions: Reversible trans-to-cis Isomerization', *ChemPlusChem*, vol. 85, no. 3, pp. 391-398. <https://doi.org/10.1002/cplu.201900575>

#### General rights

Copyright and moral rights for the publications made accessible in the public portal are retained by the authors and/or other copyright owners and it is a condition of accessing publications that users recognise and abide by the legal requirements associated with these rights.

- Users may download and print one copy of any publication from the public portal for the purpose of private study or research.
- You may not further distribute the material or use it for any profit-making activity or commercial gain
- You may freely distribute the URL identifying the publication in the public portal ?

#### Take down policy

If you believe that this document breaches copyright please contact us providing details, and we will remove access to the work immediately and investigate your claim.

# Tuneable Emission of Polyhedral Oligomeric Silsesquioxane Based Nanostructures that Self-Assemble in the Presence of Europium(III) Ions: Reversible *trans*-to-*cis* Isomerization

Valerio Cinà,<sup>[a, b]</sup> Esther Carbonell,<sup>\*[a]</sup> Luca Fusaro,<sup>[a]</sup> Hermenegildo Garcia,<sup>[c]</sup> Michelangelo Gruttadauria,<sup>[b]</sup> Francesco Giacalone,<sup>\*[b]</sup> and Carmela Aprile<sup>\*[a]</sup>

Hybrid nanostructures with switchable and reversible “blue-red-green” emission were efficiently synthesized. These nanostructures comprise polyhedral oligomeric silsesquioxanes (POSS) that behave as a nanocage that can be functionalized with terpyridine-based organic ligands, which can be easily complexed with europium (III) ions. The complexes were characterized by UV-Vis and fluorescence spectroscopy and their stoichiometry was also confirmed by <sup>1</sup>H NMR spectroscopy. In the presence of the Eu(III) ions, the octafunctionalized nanocages self-assemble to form 3D architectures that display an intense red-emission, especially in the solid state. The presence of an alkenyl group bridging the inorganic core to the

organic moiety was employed to tune the emission properties by *trans-cis* isomerization of the double bond. In the case of the octafunctionalized nanocages (O-POSS), this isomerization was monitored in the presence of Eu(III) cations and was accompanied by an evident colour change from blue (*trans*-O-POSS) to red (Eu@*trans*-O-POSS) and finally to green (*cis*-O-POSS) as consequence of the release of the metal cations. This behaviour, together with the easy dispersion of the dry powder and the possibility of coating as a film in presence of small amounts of solvent, makes the emissive solid promising for applications in materials science.

Dear Author, according to the Author's Guidelines (Wiley) the References have to be structured different. Please correct all citations exactly as follows (in the WORD-File, please. Thank you):

**Example for Journals:** a) A. Autor, B. R. Coauthor, *Z. Anorg. Allg. Chem.* **2006**, *632*, 1–5; b) A. Author, B. Coauthor, *Angew. Chem.* **2006**, *118*, 1–5; *Angew. Chem. Int. Ed.* **2006**, *45*, 1–5.

**Example for Books:** J. W. Grate, G. C. Frye in *Sensors Update, 1st ed.*, Vol. 2 (Eds.: H. Baltes, W. Göpel, J. Hesse), Wiley-VCH, Weinheim, **1996**, pp. 10–20.

[a] V. Cinà, Dr. E. Carbonell, Dr. L. Fusaro, Prof. C. Aprile  
Laboratory of Applied Material Chemistry (CMA)  
University of Namur  
61 rue de Bruxelles 5000 Namur (Belgium)  
E-mail: carmela.aprile@unamur.be

■■email missing■■

[b] V. Cinà, Prof. M. Gruttadauria, Prof. F. Giacalone  
Department of Biological  
Chemical and Pharmaceutical Sciences and Technologies  
University of Palermo  
Viale delle Scienze, Ed. 17, 90128 Palermo (Italy)  
E-mail: francesco.giacalone@unipa.it

[c] Prof. H. Garcia  
Department of Chemistry  
Instituto de Tecnología Química CSIC-UPV  
Universitat Politècnica de València  
Av. de los Naranjos s/n, 46022 Valencia (Spain)

Supporting information for this article is available on the WWW under <https://doi.org/10.1002/cplu.201900575>

**Example for Theses, Dissertations:** W. Schulz, Dissertation, Univ. Rostock, 1965.

Important: Please take attention to italics and boldface■■■

## Introduction

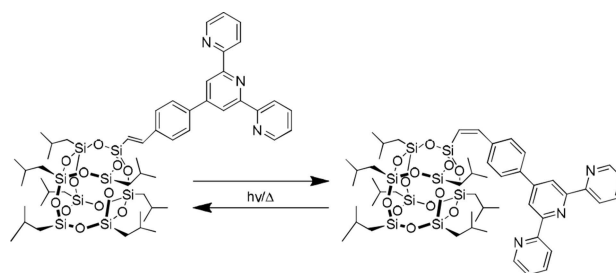
Polyhedral Oligomeric Silsesquioxane (POSS, T<sub>8</sub>) with their cubic symmetry represents an ideal building block for the construction of 3D networks. POSS exhibits an inner inorganic nanocage surrounded by eight organic moieties, which can be easily functionalized thus offering a wide range of possibilities for the synthesis of novel hybrid solids.<sup>[1]</sup> POSS nanostructures have attracted an increasing interest in recent decades. Due to their exceptional features, they found application in several fields from catalysis<sup>[2]</sup> to polymer<sup>[3]</sup> sciences. Imidazolium functionalized POSS nanostructures were efficiently employed as catalysts in the conversion of CO<sub>2</sub><sup>[4]</sup> or as support for Pd<sup>[5]</sup> nanoparticles. The exceptional chemical-physical characteristics of the nanocage (rigidity and thermal stability) were also exploited to improve the thermal stability of various polymers.<sup>[6]</sup> POSS functionalized with proper fluorophores<sup>[7]</sup> successfully acted as nanosensors for the detection of toxic industrial chemicals and chemical warfare agent simulants, whereas when the POSS rigid core is endowed with mesogenic moieties, the resulting hybrids show liquid crystal properties.<sup>[8]</sup> We recently proposed the use of POSS-based nanocages functionalized with terpyridine moieties as building unit for the efficient formation of luminescent metallopolymers in presence of Zn<sup>2+</sup> and Fe<sup>2+</sup> cations.<sup>[9]</sup> Moreover, it was also described by Cheng et al. that

when POSS structures are functionalized with fluorescent dyes, the resulting materials display an efficient emission intensity due to a combination of the improved dispersion of the fluorophore with the increased thermal stability induced by the inorganic core.<sup>[10]</sup>

Due to their peculiar luminescent properties, lanthanides trivalent ions (Ln(III)) and in particular Eu, Tb and Yb, have attracted the raising attention of the scientific community for the design of advanced functional materials<sup>[11]</sup> with possible applications in fields as different as electronics or bio-medicine.<sup>[12]</sup> The unique properties of Ln(III) include long-lived excited states, sharp line-like emission bands and large Stokes shifts. However, direct excitation of these cations is hardly obtained without laser sources due to the strongly forbidden character of the *f-f* transitions. For this reason, a species able to absorb photons at short wavelength and transfer the energy to the lanthanides, which emit lights at much longer wavelength, is often used. This process is called "antenna effect". Terpyridine-based ligands are largely employed for this purpose because of their light-harvesting antenna effect combined with high-affinity metal-bindings.<sup>[13]</sup> Moreover, it is known, that independently from the ligand used, the local chemical environment has a strong influence on the emission of Ln(III).<sup>[14]</sup>

On the other side, it would be interesting to have systems in which a controlled and tuneable emission can be obtained only via slightly chemical modification of the structure of the ligand not requiring an *ex-novo* synthesis pathway. For this purpose, the photochemical *cis-trans* isomerization of double bonds (vinyl, stilbene and azo compounds), have been the subject of a large variety of investigations. In some cases, configurational changes can be associated with different fluorescence emissions regulated by the photoisomerization process. On/off fluorescent switching<sup>[15]</sup> and photostabilization<sup>[16]</sup> via reversible *cis-trans* isomerization are also reported.<sup>[17]</sup> Photo-induced polymerization<sup>[18]</sup> as well as *cis-trans* photoisomerization studies<sup>[19]</sup> in the presence of silsesquioxane nano-cages have been reported as well.

To the best of our knowledge, photoisomerization studies in the presence of POSS-based hybrid materials, self-assembled in presence of metal ions, have never been carried out. Herein, two novel Eu<sup>3+</sup> complexes employing as ligands POSS nanostructures functionalized with one (**M-POSS**) or eight (**O-POSS**) terpyridine moieties are proposed. The reversible *trans* to *cis* isomerization of the carbon-carbon alkenyl moiety connecting the POSS nanocage to the terpyridine ligand is presented (Scheme 1). The **O-POSS** architectures display a switchable blue-green emission as consequence of the configurational changes. This switchable behaviour is even more evident in presence of Eu species. In this case a reversible "blue-red-green" emission can be easily achieved making the **O-POSS**-based Eu(III) complex an extremely promising and innovative material for emitting devices based on organic-inorganic hybrids.<sup>[20]</sup>



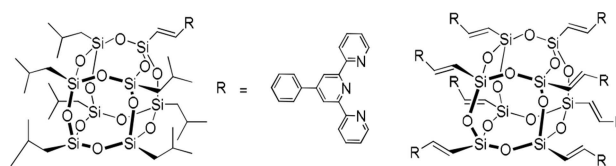
Scheme 1. *Trans-cis* isomerization of **M-POSS**.

## Results and Discussion

The synthesis of functionalized Polyhedral Oligomeric Silsesquioxane (POSS) with 4'-phenyl-2,2':6',2''-terpyridine units was achieved via Heck coupling reaction following a procedure previously described in our research group.<sup>[9]</sup> The structure of the corresponding mono- (**M-POSS**) and octa-functionalized POSS (**O-POSS**) is presented in Scheme 2. Both **M-** and **O-POSS** were characterized via <sup>1</sup>H-, <sup>13</sup>C- and <sup>29</sup>Si-NMR (see Supporting Information, Figures S1–S6).

Due to the notable light-emitting performance of the lanthanides, our attention was focused to this series of cations in order to form binary metal complexes (in presence of **M-POSS**) or 3D supramolecular assemblies (with **O-POSS**) generated through coordination of the POSS-based nanostructures with the selected metal. In particular, Eu trivalent ions were selected as target cations since they exhibit intense emission from *f-f* electronic transitions. Moreover, both POSS structures depicted in Scheme 2 display a *trans* carbon-carbon double bond that can be isomerized to the *cis* form with important implication for both emission and coordinating properties.

Prior to the investigation of the luminescent behaviour as function of the *trans-cis* isomerization, the stoichiometry of the Eu@POSS complexes (both mono- and octa-functionalized) was addressed selecting the **M-POSS** as initial benchmark. Quantitative information on the stoichiometry of the complex in function of increasing amount of Eu(III) were obtained via <sup>1</sup>H NMR titration experiments (Figure S7 in the Supporting Information). The variations of the normalized integrated areas of selected signals upon addition of increasing amounts of Eu(OTf)<sub>3</sub> are reported in Figure 1a. A progressive disappearance of the **M-POSS** free ligand contribution was observed after addition of increasing amount of Eu(III). The characteristic terpyridine signals (at 8.5 ppm), labelled with a black square, were followed for this investigation. The complete disappearance of these signals was achieved in correspondence of 0.5 eq



Scheme 2. Functionalized **M-POSS** and **O-POSS**.

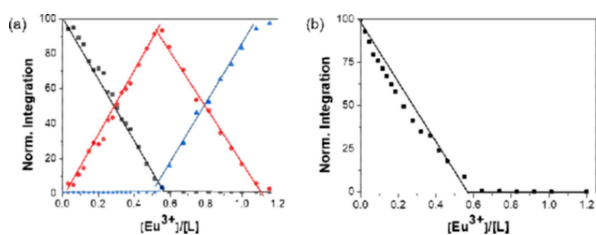


**Figure 1.** Changes in normalized integrated areas of selected signals of  $^1\text{H}$  NMR titration experiments in  $\text{CD}_3\text{Cl}:\text{CD}_3\text{CN}$  (7:3) of (a) M-POSS (b) O-POSS upon addition of 0–1.2 equivalents of  $\text{Eu}(\text{OTf})_3$  (■ = free ligand; ● = 1:2 complex; ▲ = 1:1 complex) Line connecting the point in the plot are guides for the eyes.

of  $\text{Eu}^{3+}$ . This result suggests the formation of a complex characterized by a metal to ligand stoichiometry of 1:2 (**Eu@2-MPOSS**). It should be mentioned that a novel pattern of signals corresponding to the formation of the terpyridine–Eu(III) complex (red circles) was evident immediately after the first additions of  $\text{Eu}(\text{III})$  (see Figures 1a and S7). In the presence of an excess of  $\text{Eu}(\text{OTf})_3$  an additional set of signals appears (blue triangles) which can be reasonably attributed to the formation of the 1:1 complex (**Eu@M-POSS**).

The complexation properties of the **O-POSS** in presence of  $\text{Eu}(\text{III})$  species was assessed as well.  $^1\text{H}$  NMR spectrum of **O-POSS** shows a very broad band in the aromatic region due to the  $\pi$ - $\pi$  stacking interactions (Figure S4) between the terpyridine units, as reported previously.<sup>[9]</sup> Hence, the formation of the  $\text{Eu}(\text{III})$  complex was indirectly followed by monitoring the disappearance of the  $^1\text{H}$  bands upon addition of  $\text{Eu}(\text{OTf})_3$  (Figure S8). The complete disappearance of the  $^1\text{H}$  contributions was achieved in correspondence of 0.5 equivalents  $\text{Eu}(\text{OTf})_3$  (Figure 1b) thus indicating the formation of 1:2 complex (**Eu@2O-POSS**) as previously observed when **M-POSS** was selected as ligand. Considering that lanthanides cations can accommodate up to nine coordinating atoms, the formation of complexes characterized by a metal to ligand stoichiometry of 1:2 could be considered as a consequence of the steric hindrance of the POSS nanostructure and indicates that the coordination shell of  $\text{Eu}(\text{III})$  is only partially completed by the terpyridine moieties. Interestingly, a more detailed analysis of the aliphatic region in the  $^1\text{H}$  NMR spectrum of **O-POSS** evidenced the shift of another signal at 1.9 ppm during the titration experiments (Figure S8).

This signal could be attributed to the presence of water molecules completing the first coordination shell of the  $\text{Eu}$  cations. It deserves to be mentioned that no signals corresponding to free terpyridine moieties were observed after titration. This evidence allows confirming that water plays only the role of co-ligand completing the coordination sphere and it is not able to promote the removal of the terpyridine moieties. The formation of both **M-POSS** and **O-POSS** based  $\text{Eu}(\text{III})$  complexes was also followed by monitoring the changes in the absorption and fluorescence spectra. Upon addition of  $\text{Eu}(\text{OTf})_3$  to a solution of **M-POSS**, the absorption band at 290 nm corresponding to the  $\pi$ - $\pi^*$  transition of the terpyridine decreases remarkably. Concomitantly, the appearance of a

novel absorption band above 330 nm was progressively observed (see Figure 2a). These absorption bands can be attributed to the metal/ligand complex. A plateau was reached in correspondence of a M/L ratio equal to 0.5 (inset Figure 2a) further confirming the formation of the **Eu@2 M-POSS**.

The fluorescence spectra followed a similar trend. As expected, the emission band of the terpyridine in the **M-POSS** ( $\lambda_{\text{max}}=365$  nm) was completely quenched upon addition of 0.5 equivalents of metal cations (see Figure 2b). As a direct consequence of complex formation, a new emission band at  $\lambda_{\text{max}}$  ca. 455 nm was observed. This broad emission band can be attributed to the ligand-centred transitions. However, under the selected conditions, the characteristic  $\text{Eu}(\text{III})$  emission (in the region between 550–700 nm) was not detected. This behaviour could be attributed to the incomplete energy transfer from the terpyridine to the europium and/or the influence of the solvent polarity as well as the presence of water molecules. **M-POSS** possess seven hydrophobic isobutyl groups surrounding the nanocage with consequent generation of a “hydrophobic shell” influencing the self-association process.<sup>[21]</sup> In order to better understand the reason behind the absence of this emission, a novel set of experiments employing a mixture of solvents of different polarity ( $(\text{CH}_3\text{CN}$  (97%): $\text{CH}_2\text{Cl}_2$  (3%)) was performed as well. Figure S9 shows a non-resolved emission centred at 617 nm clearly visible in the novel mixture of solvent thus confirming the role played by the solvent on the emission of **M-POSS** structures.

However, a different behaviour with an improved emission should be expected in presence of **O-POSS** based ligands in which the isobutyl groups are replaced by terpyridine moieties.

As expected, the addition of  $\text{Eu}(\text{OTf})_3$  causes a progressive decrease of the terpyridine emission band ( $\lambda_{\text{max}}=390$  nm) with a complete disappearance achieved in correspondence of 0.5 equivalents of metal (formation of 1:2 complex, Figure 3a).

Also in this case a broad emission ligand centred band was still present. It is noteworthy that once the complex was formed, the characteristic  $\text{Eu}(\text{III})$  line-like emission was clearly observed. The five sharp emission peaks at 580, 591, 617, 650 and 698 nm (inset Figure 3a), were assigned to the  $^5\text{D}_0 \rightarrow ^7\text{F}_J$  ( $J=0, 1, 2, 3, 4$  and 5) transitions, with the most intense at 617 nm corresponding to the  $^5\text{D}_0 \rightarrow ^7\text{F}_2$  emission. It is important to underline, that under the highly diluted conditions ( $10^{-7}$  M) employed to monitor the absorption and emission features of

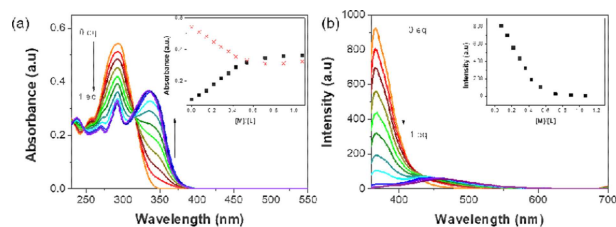


**Figure 2.** (a) UV-vis absorption spectra of **M-POSS** in  $\text{CH}_2\text{Cl}_2$  ( $1.3 \times 10^{-5}$  M) upon titration with  $\text{Eu}(\text{OTf})_3$  in  $\text{CH}_3\text{CN}$  ( $1.4 \times 10^{-3}$  M). Inset shows the normalized absorption changes at 290 nm (red crosses) and 330 nm (black squares). (b) Emission spectra of **M-POSS** in  $\text{CH}_2\text{Cl}_2$  upon titration with  $\text{Eu}(\text{OTf})_3$ : 0 eq.–1 eq.  $\lambda_{\text{exc}}=310$  nm  $\text{OD}_{315}$  nm = 0.27 slits 2.5–5 and band pass filter (360–100 nm). Inset shows the fluorescence intensity at 366 nm.

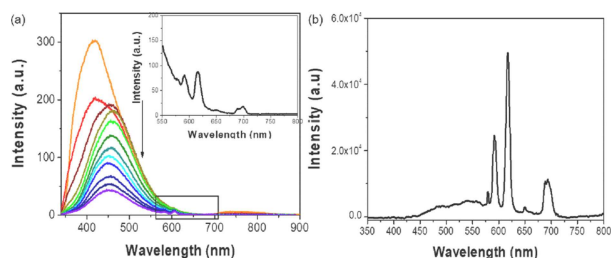


**Figure 3.** (a) Emission spectra of **O-POSS** [ $1 \times 10^{-5}$  M] in  $\text{CH}_2\text{Cl}_2$  upon addition of  $\text{Eu}(\text{OTf})_3$  [ $1.4 \times 10^{-3}$  M] in  $\text{CH}_3\text{CN}$  ( $\lambda_{\text{ex}} = 313$  nm OD = 0.15 slits 5 nm). Inset shows the characteristic  $\text{Eu}(\text{III})$  line-like emission. (b) Emission spectra of the **Eu@O-POSS** in solid state.

the **Eu@O-POSS** complex a perfectly homogeneous and transparent solution was always obtained during the titration experiments. UV-Vis absorption spectra of **O-POSS** in  $\text{CH}_2\text{Cl}_2$  upon titration with  $\text{Eu}(\text{OTf})_3$  are reported in Figure S10. The use of other mixtures of solvents was not possible due to the poor solubility of both **O-POSS** and metal precursors in the same medium.

This solution was characterized by a red emission evident also to the naked eyes. However, precipitation of the **Eu@O-POSS** assembled structure can be easily achieved in more concentrated solution.

Hence, solid state emission properties of the **Eu@O-POSS** complex were evaluated as well. As can be clearly seen in Figure 3b, the emission spectrum of the solid display excellent features characterized by a strong emission intensity as well as by a narrow half emission width of c.a. 10 nm. Moreover, the decrease of the intensity of the emission band of the complexed ligand suggests that the energy transfer from the terpyridine ligands to the  $\text{Eu}(\text{III})$  is more efficient in the solid state. The more intense emission of **Eu@O-POSS** complex compared to the **M-POSS**-based structures can be considered as a consequence of the increased local concentration of the terpyridine surrounding the nanocage and constitute an indication of the important role played by the 3D metallopolymeric network protecting  $\text{Eu}(\text{III})$  against non-radiative deactivation. These differences in the emission arising from the different environments in the assembled coordination complexes could be due to the molecular packing inducing higher emission.<sup>[22]</sup>

Transmission electron microscopy investigation of the self-assembled **Eu@O-POSS** structures was performed as well. As expected, this study revealed that the final solid is composed by a non-ordered polymeric network (Figure S11). We can consider the self-assembled organization as a disordered 3D architecture in which various **O-POSS** are interconnected via the  $\text{Eu}(\text{III})$  cations. Once proved the emission properties of the **Eu@O-POSS** an investigation of the *trans-cis* reversible isomerization was performed. It is well known that UV light irradiation may promote *trans* to *cis* isomerization of the alkenyl group. The formation of the *cis*-isomer was monitored via  $^1\text{H}$  NMR spectroscopy selecting the **M-POSS** as target molecule. The formation of an almost equimolecular mixture of *cis* and *trans* isomers was achieved through irradiation of the *trans*-**M-POSS**

at 356 nm. As can be clearly seen in Figure 4, the initial  $^1\text{H}$  NMR spectrum displays, in the vinyl region, only one signal at 6.22 ppm (coupling constant  $J = 19.1$  Hz) corresponding to the alkenyl group in *trans* configuration. After irradiation, a novel signal at 5.70 ppm (coupling constant  $J = 15.2$  Hz) corresponding to the *cis* form appears together with a series of signals in the aromatic part of the spectrum.

Once proved the possibility to form the *cis*-**M-POSS** structure, the *trans*-to-*cis* photoisomerization process was followed at different irradiation times via UV-visible and fluorescence spectroscopies. Upon irradiation, a decrease of the absorbance of the UV-Visible band centred at 290 nm and the concomitant appearance of a shoulder were observed (Figure S12).

A more evident transition was clearly distinguished in the fluorescent spectra. An almost complete disappearance of the emission band of *trans*-**M-POSS** at 366 nm together with the appearance of a novel emission band at 460 nm (attributed to the *cis* form) was observed after 60 minutes of irradiation at 356 nm (Figure 5 and S13). Interestingly, under the conditions employed in the fluorescence experiments, a total *trans*-to-*cis* conversion was achieved after 1 h irradiation. The reversibility of the isomerization process was obtained via thermal treatment, heating the **M-POSS** solution at  $50^\circ\text{C}$  during 1 h (Figure 5a). Indeed, after thermal treatment at  $50^\circ\text{C}$  the band at

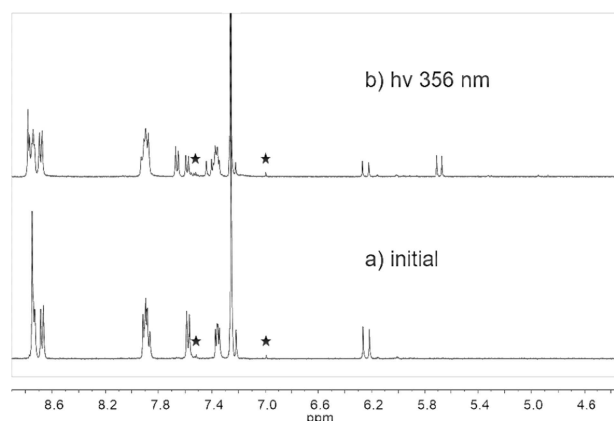


**Figure 4.**  $^1\text{H}$  NMR spectrum in  $\text{CDCl}_3$  of **M-POSS** (a) before and (b) after irradiation at 356 nm.  $\star$  indicates the  $^{13}\text{C}$  satellites.

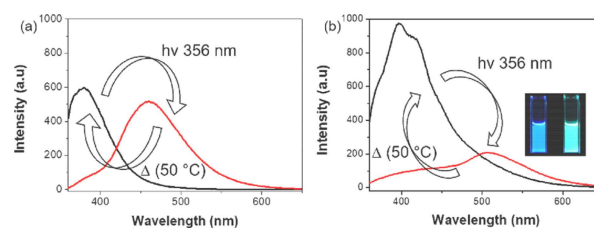


**Figure 5.** (a) Reversible emission spectra of *trans*-**M-POSS** solution (black line) and *cis*-**M-POSS** (red line) ( $1.0 \times 10^{-5}$  M) in dichloromethane registered at  $\lambda_{\text{ex}} = 314$  nm slits 2.5, 5 nm (bandpass filter 360–1100 nm). (b) Emission spectra of **O-POSS** before and after irradiation at 356 nm. Black line: *trans*-**O-POSS** solution and red line: *cis*-**O-POSS**  $C = 1.2 \times 10^{-5}$  M;  $\lambda_{\text{ex}} = 314$  nm; slits 5, 10. Inset shows the digital photograph of the cuvette at initial and after 60 min taken under UV light at 356 nm.

460 nm disappeared while the contribution at 366 nm was completely restored. The process can be repeated multiple times with highly consistent results. Excitation spectra of the M-POSS at the maximum of the respective emissions (370 nm for the *trans*- form and 460 nm for the *cis*- form) were recorded being practically coincident with the corresponding absorption spectra of *trans*- and *cis*- configurations respectively (Figure S14) indicating that the detected emission corresponds to the *trans*- and the *cis*- forms without observations of the excimers photoisomerization process of O-POSS at different irradiation formation in these conditions. Analogous irradiation experiments were carried out in presence of O-POSS. The times were followed by UV-Visible and fluorescence spectroscopies. *Trans*-to-*cis* photoisomerization occurred under UV light irradiation also in presence of the O-POSS nanostructures. In agreement with the previously described behaviour of M-POSS, a decrease of the absorption band of the ligand (ca. 285 nm) and the appearance of a shoulder was observed (see Figure S15). Moreover, the emission band of the ligand was quenched almost completely and a novel broad emission band, corresponding to the *cis* form, appeared at 510 nm (Figure 5b). The broader emission band of the *cis*-O-POSS compared to the *trans*- isomer could be ascribed to the presence of excimers favoured by the *cis*-configuration of the double bond. It is important to underline that the silsesquioxane nano-cages constitute a photochemical inert molecular scaffold and the emission properties of both M- and O-POSS structures should be ascribed to the presence of the terpyridine moieties. Interestingly, in the case of O-POSS nanostructures the *trans* to *cis* isomerization was accompanied by an evident change in colour that passed from blue (*trans*-O-POSS) to green (*cis*-O-POSS). As previously observed for the M-POSS, also the octa-functionalized analogues display a reversible isomerization.

Due to the relevant interest that could present a tuneable photochromism of the self-assembled 3D network, the isomerization process of the Eu@O-POSS complex was followed as well via UV-Visible and fluorescence spectroscopies. It is worth highlighting that under UV irradiation the Eu@O-POSS complexes release almost completely the coordinated Eu(III) ions. As we can observe in the Figure 6, the characteristic Eu(III) emission bands disappeared after 1 h irradiation. This behaviour can be ascribed to elevate steric hindrance of the O-POSS in the *cis* forms hindering the coordination of the metal centre. Changes in fluorescence emission of the Eu@O-POSS under UV light exposure can be detected also at naked eyes (Scheme 3).

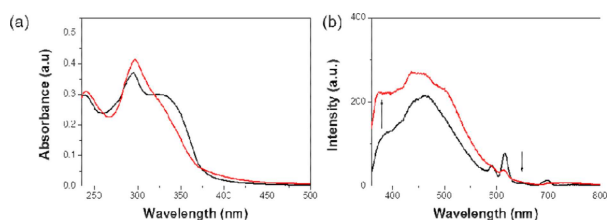
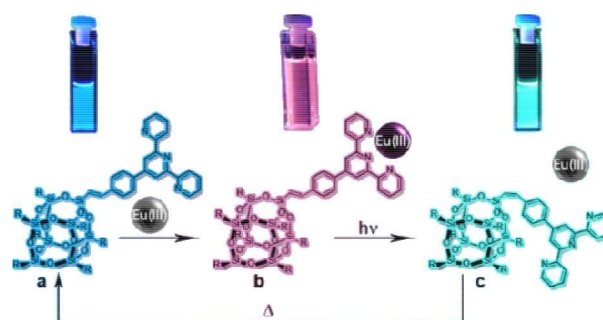


**Figure 6.** (a) UV-visible and (b) emission spectra of Eu@O-POSS (1:2) before (black line) and after irradiation (red line) at 356 nm for 60 minutes. [O-POSS] =  $1.3 \times 10^{-5}$  M;  $\lambda_{\text{ex}}$  = 314 nm; slits 5, 10; (bandpass filter 360–1100 nm).



**Scheme 3.** Schematic representation of the tuneable emission of (a) *trans*-O-POSS in dichloromethane solution; (b) Eu@*trans*-O-POSS; (c) *cis*-O-POSS after irradiation at 356 nm (60 minutes) under UV lamp. (R = phenyl-2,2':6',2''-terpyridine).

*Trans*-O-POSS (a) displays an evident blue emission, after formation of the Eu@*trans*-O-POSS complex a shift through the red is clearly observed (b), UV-irradiation of the Eu@*trans*-O-POSS causes the release of the Eu(III) ions due to the formation of the *cis*-O-POSS isomer whose free (non-complexed) form emits in the green (c). After thermal treatment the *cis*-O-POSS can be completely converted in the *trans* isomer and the cycle can be repeated without detrimental effect on O-POSS nanostructure.

Moreover, in presence of small amount of solvent the Eu@O-POSS can be easily shaped as a film as illustrated in Figure 7. This behaviour can open the doors to application in materials science.

## Conclusion

The absorption and emission properties of two novel silsesquioxane-based Eu complexes were investigated. The stoichiometry of the complexes (Eu@2M-POSS and Eu@2O-POSS) was evaluated via  $^1\text{H}$  NMR as well as UV-Vis and fluorescence titration experiments. The solutions of Eu@2O-POSS display a bright-red luminescence under UV light at room temperature and an even more intense emission can be achieved in solid state. Interestingly both M- and O-POSS nanostructures display



**Figure 7.** Film of the acronym of the University of Namur designed employing the *trans*-O-POSS (first two letters on the right), Eu@*trans*-O-POSS (letters in the middle) and *cis*-O-POSS (last two letters on the right) under UV lamp (356 nm).

a reversible *trans* to *cis* isomerization of the carbon–carbon double bond linking the silsesquioxane core to the terpyridine moieties. In the case of **O-POSS** nanocages this isomerization was monitored also in presence of Eu(III) cations and was accompanied by an evident modification of the colour which passed from blue (*trans*-**O-POSS**) to red (**Eu@trans-O-POSS**) and finally to green (*cis*-**O-POSS**) as consequence of the release of the metal cations. After thermal treatment, the *cis*-**O-POSS** can be completely converted in the *trans* isomer and the cycle can be repeated without detrimental effect on **O-POSS** nanostructure. This switchable and reversible “blue-red-green” emission together with the easy dispersion, solubility in organic solvents and the possibility of forming films makes the emitting solid promising for applications in materials science and in particular in the preparation of advanced light emitting devices.

## Experimental Section

**Materials and method:** Monovinyl–isobutyl substituted POSS (MV), Octavinyl POSS (OV), DMF anhydrous, Et<sub>3</sub>N (99.5%), Eu(III) triflate (99.999%) were purchased from Sigma Aldrich. 4'-(4-Bromophenyl)-2,2':6',2''-terpyridine, palladium acetate, tris(2-methylphenyl) phosphine were purchased from TCI chemicals. Acetonitrile (CH<sub>3</sub>CN) and dichloromethane (DCM) used for the spectrofluorometric measurements were of spectroscopic grade and these were purchased from Carl Roth. Quantitative <sup>1</sup>H NMR experiments were performed at 25 °C on a Varian V NMR spectrometer. UV-visible measurements were performed on Cary 5000 Spectrophotometer (Varian) and fluorescent measurements on Cary Eclipse (Agilent technologies). The measurements were carried out using 10 mm suprasil quartz cuvettes from Hellma Analytics. Irradiation test were performed with an ASASHI SPECTRA Xenon Light Source 300 W MAX-303.

**Synthesis M-POSS:** To an oven-dried, double neck 50 mL flask under flowing N<sub>2</sub>, 400 mg of MV (0.42 mmol), 10.8 mg of palladium acetate, 29.2 mg of tris(2-methylphenyl)phosphine (0.096 mmol), 280 mg of 4'-(4-bromophenyl)-2, 2':6', 2''-terpyridine (0.72 mmol), 14 mL of DMF anhydrous and 4 mL of Et<sub>3</sub>N were added. The reaction mixture was heated at 100 °C for 3 days under N<sub>2</sub> atmosphere. After that, the mixture was cooled at room temperature and filtered to remove the palladium metal. The filtrate was cooled down precipitating the **M-POSS**.

**M-POSS**, white powder. **Yield: 80%**. <sup>1</sup>H-NMR (400 MHz, CDCl<sub>3</sub>) δ (ppm) = 0.69–0.62 (m, 14H), 0.95–1.00 (m, 42H), 1.81–1.95 (m, 7H), 6.27–6.22 (d, 1H), 7.27–7.22 (d, 1H), 7.37–7.34 (t, 2H), 7.59–7.57 (d, 1H), 7.92–7.86 (m, 4H), 8.69–8.67 (d, 2H), 8.74–8.73 (d, 2H), 8.75 (s, 2H). <sup>13</sup>C-NMR (100 MHz, CDCl<sub>3</sub>) δ (ppm) = 22.60, 23.96, 25.82, 118.77, 119.81, 121.47, 123.96, 127.43, 127.61, 136.99, 138.39, 138.65, 147.38, 149.24, 149.77, 156.06, 156.30. MAS <sup>29</sup>Si-NMR (99.3 MHz) δ (ppm) = –68.27, –80.17. Elemental analysis (%) for C<sub>51</sub>H<sub>79</sub>N<sub>3</sub>O<sub>12</sub>Si<sub>8</sub>; calculated: C = 53.23, H = 6.92, N = 3.65; found: C = 52.45, H = 6.79, N = 3.22.

**Synthesis O-POSS:** To an oven-dried, double neck 50 mL flask under flowing N<sub>2</sub>, 135 mg of OV (0.21 mmol), 20.8 mg of palladium acetate (0.09 mmol), 58 mg of tris(2-methylphenyl)phosphine (0.018 mmol), 1 g of 4'-(4-bromophenyl)-2, 2':6', 2''-terpyridine (2.57 mmol), 14 mL of DMF anhydrous and 4 mL of Et<sub>3</sub>N were added. The reaction mixture was heated at 100 °C for 7 days under N<sub>2</sub> atmosphere. After that, the mixture was cooled and filtered to remove the Pd<sup>0</sup> and then precipitated in 50 mL of deionized water. The precipitate was, for first, washed with water (2 × 25 mL)

sonicating in a bath and centrifuging 10 minutes at 4500 rpm. The same procedure was repeated washing the solid with acetonitrile (5 × 25 mL), then with methanol (5 × 25 mL) and finally with acetone (2 × 25 mL). **O-POSS** was obtained as a pale brown powder. Yield: 68%. MAS <sup>29</sup>Si NMR (99.3 MHz) δ (ppm) = –80.29. Elemental analysis (%) for C<sub>51</sub>H<sub>79</sub>N<sub>3</sub>O<sub>12</sub>Si<sub>8</sub>; calculated: C = 71.48, H = 4.17, N = 10.87; found: C = 67.04, H = 3.99, N = 9.78.

**Synthesis Eu@20-POSS:** In a single-neck 50 mL flask 50 mg of O-POSS (0.016 mmol), 39 mg of Eu (III) triflate (0.065 mmol) and 20 mL of a mixture of DCM and CH<sub>3</sub>CN (65%:35%) were added. The mixture was cooled at 50 °C for 24 h. After this time, the volume of the mixture was reduced by evaporation under reduced pressure and a pale yellow precipitate was collected under vacuum. The solid was washed on the filter with DCM and CH<sub>3</sub>CN and dried under vacuum.

**Irradiation procedure:** Irradiation tests for <sup>1</sup>H-NMR were performed in “5 mm Thin Wall Natural Quartz NMR Sample Tubes” from NORELL. Absorption and emission experiments were performed in 10 mm suprasil quartz cuvettes from Hellma Analytics. All the irradiation tests were carried out by placing the samples at a distance of 21 cm from the UV source.

## Acknowledgements

The authors acknowledge the University of Palermo and the University of Namur. V.C. gratefully acknowledges the University of Palermo and University of Namur for a co-funded PhD fellowship.

## Conflict of Interest

The authors declare no conflict of interest.

**Keywords:** europium · isomerization · luminescence · self-assembly · silsesquioxanes

- [1] P. P. Pescarmona, C. Aprile, S. Swaminathan, in *New and Future Developments in Catalysis* (Ed.: S. L. Suib), Elsevier, 2013.
- [2] a) R. Duchateau, W. J. van Meerendonk, S. Huijser, B. B. P. Staal, M. A. van Schilt, G. Gerritsen, A. Meetsma, C. E. Koning, M. F. Kemmere, J. T. F. Keurentjes, *Organometallics* 2007, 26, 4204–4211; b) R. Kunthom, T. Jaroentomeechai, V. Ervithayasuporn, *Polym. J.* 2017, 108, 173–178; c) K. Wada, M. Nakashita, T. Mitsudo, *Chem. Commun.* 1998, 133–134.
- [3] a) R. Y. Kannan, H. J. Salacinski, J.-E. Ghanavi, A. Narula, M. Odlyha, H. Peirovi, P. E. Butler, A. M. Seifalian, *Plast. Reconstr. Surg.* 2007, 119, 1653–1662; b) S. B. Rizvi, S. Y. Yang, M. Green, M. Keshtgar, A. M. Seifalian, *Bioconjugate Chem.* 2015, 26, 2384–2396; c) C. Zhang, F. Babonneau, C. Bonhomme, R. M. Laine, C. L. Soles, H. A. Hristov, A. F. Yee, *J. Am. Chem. Soc.* 1998, 120, 8380–8391.
- [4] a) L. A. Bivona, O. Fichera, L. Fusaro, F. Giacalone, M. Buaki-Sogo, M. Gruttadauria, C. Aprile, *Catal. Sci. Technol.* 2015, 5, 5000–5007; b) C. Calabrese, L. F. Liotta, F. Giacalone, M. Gruttadauria, C. Aprile, *ChemCatChem*, 2019, 11, 560–567.
- [5] a) L. A. Bivona, F. Giacalone, E. Carbonell, M. Gruttadauria, C. Aprile, *ChemCatChem* 2016, 8, 1685–1691.
- [6] A. Tsuchida, C. Bolln, F. G. Sernetz, H. Frey, R. Mülhaupt, *Macromolecules* 1997, 30, 2818–2824.
- [7] C. Hartmann-Thompson, D. L. Keeley, K. M. Pollock, P. R. Dvornic, S. E. Keinath, M. Dantus, T. C. Gunaratne, D. J. Le Captain, *Chem. Mater.* 2008, 20, 2829–2838.
- [8] G. H. Mehl, I. M. Saez, *Appl. Organomet. Chem.* 1999, 13, 261–272.

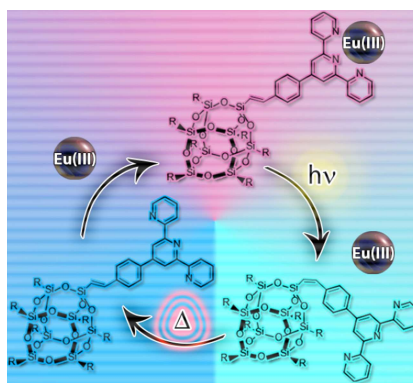
- [9] E. Carbonell, L. A. Bivona, L. Fusaro, C. Aprile, *Inorg. Chem.* 2017, 56, 6393–6403.
- [10] C.-C. Cheng, Y.-L. Chu, C.-W. Chu, D.-J. Lee, *J. Mater. Chem. C* 2016, 4, 6461–6465.
- [11] a) P. Escribano, B. Julián-López, J. Planelles-Aragó, E. Cordoncillo, B. Viana, C. Sanchez, *J. Mater. Chem.* 2008, 18, 23–40; b) L. Li, S. Feng, H. Liu, *J. Ceram. Soc. Jpn.* 2015, 123, 719–724; c) L. Li, S. Feng, H. Liu, *RSC Adv.* 2014, 4, 39132–39139.
- [12] S. S. Syamchand, G. Sony, *J. Lumin.* 2015, 165, 190–215.
- [13] a) U. S. Schubert, A. Winter, G. R. Newkome, in *Terpyridine-Based Materials*, Wiley-VCH Verlag GmbH & Co. KGaA, 2011, pp. 129–197; b) O. Kotova, S. Comby, C. Lincheneau, T. Gunnlaugsson, *Chem. Sci.* 2017, 8, 3419–3426.
- [14] V. Bekiari, P. Lianos, *J. Lumin.* 2003, 101, 135–140.
- [15] a) J. W. Chung, S.-J. Yoon, B.-K. An, S. Y. Park, *J Phys Chem C* 2013, 117, 11285–11291; b) C. Dugave, L. Demange, *Chem. Rev.* 2003, 103, 2475–2532.
- [16] P. P. Lima, M. M. Nolasco, F. A. A. Paz, R. A. S. Ferreira, R. L. Longo, O. L. Malta, L. D. Carlos, *Chem. Mater.* 2013, 25, 586–598.
- [17] L.-R. Lin, H.-H. Tang, Y.-G. Wang, X. Wang, X.-M. Fang, L.-H. Ma, *Inorg. Chem.* 2017, 56, 3889–3900.
- [18] W. Yang, Y. Gan, X. Jiang, H. Liu, *Eur. J. Inorg. Chem.* 2015, 2015, 99–103.
- [19] Y. Liu, W. Yang, H. Liu, *Chem. Eur. J.* 2015, 21, 4731–4738.
- [20] a) M. Bian, Y. Wang, X. Guo, F. Lv, Z. Chen, L. Duan, Z. Bian, Z. Liu, H. Geng, L. Xiao, *J. Mater. Chem. C* 2018, 6, 10276–10283; b) D. Zych, A. Slodek, M. Matussek, M. Filapek, G. Szafraniec-Gorol, S. Krompiec, S. Kotowicz, M. Siwy, E. Schab-Balcerzak, K. Bednarczyk, M. Libera, K. Smolarek, S. Maćkowski, W. Danikiewicz, *ChemistrySelect* 2017, 2, 8221–8233.
- [21] H.-L. Au-Yeung, S. Y.-L. Leung, A. Y.-Y. Tam, V. W.-W. Yam, *J. Am. Chem. Soc.* 2014, 136, 17910–17913.
- [22] a) J. Andres, A.-S. Chauvin, *Eur. J. Inorg. Chem.* 2010, 2010, 2700–2713; b) V. Divya, R. O. Freire, M. L. P. Reddy, *Dalton Trans.* 2011, 40, 3257–3268; c) Z.-M. Zhang, F.-F. Han, R. Zhang, N. Li, Z.-H. Ni, *Tetrahedron Lett.* 2016, 57, 1917–1920.

---

Manuscript received: September 22, 2019  
Revised manuscript received: November 11, 2019

## FULL PAPERS

**Colourful switch:** Polyhedral oligomeric silsesquioxane (POSS)/terpyridine hybrid ligands efficiently complex Eu(III) ions. The emission of the complexes can be tuned *trans-cis* isomerization of the bridging alkenyl group. Isomerization of an octahedrally functionalized POSS (O-POSS) was accompanied by a modification of the emission colour which passed from blue (*trans*-O-POSS) to red (Eu@*trans*-O-POSS) and finally to green (*cis*-O-POSS) as consequence of the release of the Eu(III) ion. After thermal treatment, the *cis*-O-POSS can be converted again to the *trans* isomer.



V. Cinà, Dr. E. Carbonell\*, Dr. L. Fusaro, Prof. H. Garcia, Prof. M. Gruttadauria, Prof. F. Giacalone\*, Prof. C. Aprile\*

1 – 8

**Tuneable Emission of Polyhedral Oligomeric Silsesquioxane Based Nanostructures that Self-Assemble in the Presence of Europium(III) Ions: Reversible *trans*-to-*cis* Isomerization**



Tuneable emission and reversible *trans*-to-*cis* isomerization of polyhedral oligomeric silsesquioxane based nanostructures that self-assemble in the presence of Eu(III) ions (Giacalone, Aprile et al.)

@UNamur @udepalermo @UPV

Share your work on social media! ChemPlusChem has added Twitter as a means to promote your article. Twitter is an online microblogging service that enables its users to send and read short messages and media, known as tweets. Please check the pre-written tweet in the galley proofs for accuracy. If you, your team, or institution have a Twitter account, please include its handle @username. Please use hashtags only for the most important keywords, such as #catalysis, #nanoparticles, or #proteindesign. The ToC picture and a link to your article will be added automatically, so the tweet text must not exceed 250 characters. This tweet will be posted on the journal's Twitter account (follow us @ChemPlusChem) upon publication of your article in its final (possibly unpaginated) form. We recommend you to re-tweet it to alert more researchers about your publication, or to point it out to your institution's social media team.

#### ORCID (Open Researcher and Contributor ID)

Please check that the ORCID identifiers listed below are correct. We encourage all authors to provide an ORCID identifier for each coauthor. ORCID is a registry that provides researchers with a unique digital identifier. Some funding agencies recommend or even require the inclusion of ORCID IDs in all published articles, and authors should consult their funding agency guidelines for details. Registration is easy and free; for further information, see <http://orcid.org/>.

Valerio Cinà  
Dr. Esther Carbonell  
Dr. Luca Fusaro  
Prof. Hermenegildo Garcia  
Prof. Michelangelo Gruttadauria  
Prof. Francesco Giacalone  
Prof. Carmela Aprile <http://orcid.org/0000-0002-3193-3239>